Following the DNA Ligation of a Single Duplex Using Atomic Force Microscopy

Eung-Sam Kim,[†] Jung Sook Kim,[‡] Yoonhee Lee,[‡] Kwan Yong Choi,[†,§] and Joon Won Park[†,‡,*]

[†]School of Interdisciplinary Bioscience and Bioengineering, [‡]Department of Chemistry, Division of Integrative Biosciences and Biotechnology, and [§]Department of Life Science, Division of Molecular and Life Sciences, Pohang University of Science and Technology, San 31 Hyoja-dong, Pohang, 790-784, South Korea

ABSTRACT

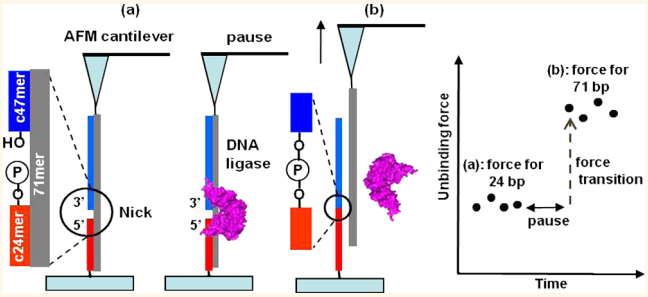

Nick-sealing of a single DNA duplex was studied with the use of atomic force microscopy (AFM). To form a nick between a 47mer DNA and a 24mer DNA, the complementary 71mer template DNA immobilized on an AFM tip was hybridized with the 47mer DNA and brought into contact with the 24mer DNA on a substrate surface. The AFM tip and substrate surface were modified with dendron molecules to ensure the formation of a single DNA duplex. When a single nick in the DNA duplex was sealed by DNA ligase during a pause, an increase in the unbinding force was observed after the pause. The change from 24.0 ± 4.4 piconewtons (pN) to 62.8 ± 14.6 pN matched well with the resulting DNA length (71 bp). Additionally, a 30 s pause showed a 3-fold higher nick-sealing probability (60%) than a 10 s pause, while the probability did not increase with a 120 s pause. In the presence of free 47mer DNAs in solution, the single nick-sealing event could be repeated at other positions.

KEYWORDS: DNA ligation · single-molecule manipulation · atomic force microscopy · unbinding force measurement · dendron-modified surface

The enzyme-assisted patterning with atomic force microscopy (AFM)[1,2] has allowed the controlled placement of target molecules onto a solid surface at micrometer- or nanometer-scale precision. The enzymatic nanolithography could provide a topographic pattern when the product from the enzymatic reaction was deposited *de novo* along the movement of the AFM tip.[3,4] A negative pattern was achieved by removing preexisting biomolecules or converting them into smaller ones with an AFM tip where an active enzyme was immobilized.[5−7] Recently, for the high-throughput and flexible molecular printing, dip-pen nanolithography (DPN)[8] and microcontact printing[9] have been integrated into multiplexed DPN and polymer-pen lithography.[10] The generated patterns were visualized by AFM or fluorescence microscopy after completing serial or parallel nanolithography.[11,12]

As a smaller feature size of the pattern is desired, well-controlled approaches are required to implement the transfer of a single molecule to a designated position onto a substrate surface. While AFM has been useful for studying the single-molecular event[13−18] as well as other single-molecular force spectroscopic techniques,[19] AFM can transfer a single molecule to a designated position. Kufer *et al.* demonstrated the single-molecule cut-and-paste of DNA with AFM[20] and monitored the bottom-up molecular assembly in real time with total internal reflection microscopy.[21] We previously reported that dendron molecules could control the lateral spacing between the immobilized biomolecules on both the substrate surface and AFM tip.[22,23] Thus, a modified AFM tip could pick a single copy of DNA and single ferritin reliably.[23,24]

Here, we report the ligation reaction of a single duplex with the use of AFM. An AFM tip and a substrate surface modified with dendrons were placed close to form a single nick in the DNA duplex in the presence of DNA ligase (Scheme 1).[25,26] The approach by which the enzymatic elongation of a single DNA strand at a position where the AFM tip brings a template DNA for ligation paves a new avenue leading to positive nanopatterning of single-molecule precision.

RESULTS AND DISCUSSION

When a 27-acid dendron-modified AFM tip tethering the 71mer DNA was employed to measure the interaction with c24mer

* Address correspondence to jwpark@postech.ac.kr.

Received for review March 19, 2012 and accepted June 11, 2012.

Published online June 11, 2012
10.1021/nn301200k

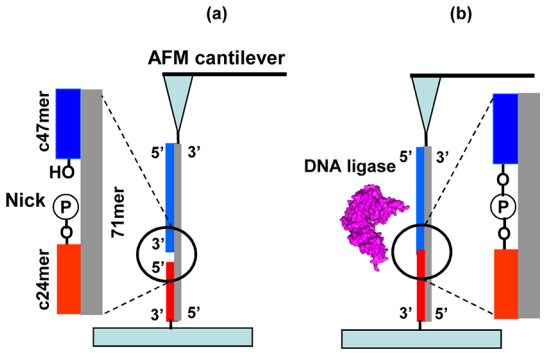

Scheme 1. Single nick-sealing event using atomic force microscopy. (a) Formation of a single DNA nick between c24mer and c47mer DNA. An AFM tip with the hybridized 71mer/c47mer DNA approaches the c24mer DNA (5′-PO_4) immobilized on the substrate surface. (b) During a given pause time, T4 DNA ligase recognizes the nick and produces a phosphodiester bond between the 5′-PO_4 and 3′-OH in the nick, yielding a ligated c71mer DNA. After the pause, the AFM tip is retracted upward to separate the 71mer from the ligated c71mer, and the force−distance curve shows an increase in the unbinding force

DNA, the most probable unbinding force values determined from the single-peaked curves were 28.4 ± 5.1 piconewtons (pN) (Figure 1A) and 28.7 ± 5.5 pN (Figure S1A) on the 9-acid dendron surface and high-density surface, respectively. The proportions of single-peaked and double-peaked unbinding events among the total measurements were 50% and 39%, respectively, on the high-density surface. In contrast, the single-peaked unbinding event became dominant to reach 86% for the former case, whereas the percentage of the double-peaked unbinding event decreased to 5%. The multipeaked unbinding events were rarely observed on the dendron-modified surface. The unbinding force values for the c71mer DNA were 57.2 ± 7.6 pN (Figure 1B) and 55.3 ± 7.0 pN (Figure S1B) on the dendron-modified surface and the high-density surface, respectively, when the single-peaked curves were analyzed. The percentages of single-peaked and double-peaked curves on the high-density surface were 41% and 38%, respectively, whereas those on the dendron-modified surface were 79% and 11%. The force measurement for both the c24mer (5′-PO_4) and c24mer (5′-OH) DNAs immobilized on the dendron-modified surface was carried out with an AFM tip tethering the 71mer/c47mer DNA to investigate the effect of terminal groups on the unbinding force (Figures 1C and S1C). The c24mer DNA (5′-PO_4) showed an unbinding force of 27.2 ± 5.0 pN, and the c24mer DNA (5′-OH) displayed 26.6 ± 5.3 pN from the analysis of the single-peaked curves (Figure S2 and Table S1). While the former case showed a slightly higher value than the latter one, the difference was too small to be significant. Therefore, it can be said that the end group does not alter the unbinding force as long as the group is not the one that deters the base pairing through steric or electronic effects.

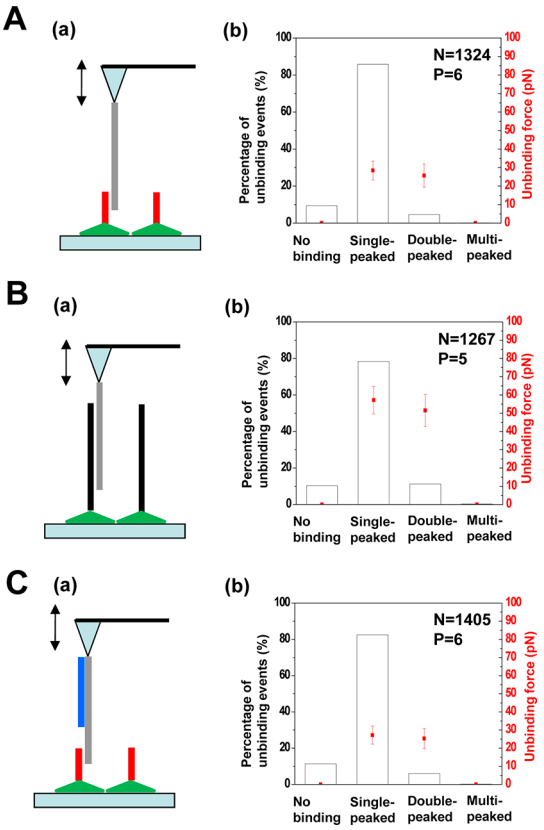

Figure 1. Unbinding events on the 9-acid dendron surface. The 71mer DNA was tethered on an AFM tip modified with the 27-acid dendron. Force measurement at five or six different points was performed repeatedly more than 100 times per point at which specific unbinding forces were recorded. The green triangle on the surface represents the 9-acid dendron molecule. (A) Measurement of unbinding forces for the c24mer (5′-PO_4) DNA (a) and probability and distribution (b). (B) Measurement of unbinding forces for the c71mer DNA (a) and probability and distribution (b). (C) Measurement of unbinding forces for the c24mer (5′-PO_4) DNA using 71mer/c47mer DNA tethered on the AFM tip (a) and probability and distribution (b). *N* and *P* values denote the total number of measurements and the number of examined points, respectively. The *y*-axis on the right-hand side is the unbinding force value, and dots in the graph represent the most probable force value in each category (single-peaked, double-peaked, or multipeaked). The probability of observing the multipeaked curve on the 9-acid dendron-modified surface was less than 1%.

Surface modification of the AFM tip and substrate surface with 27-acid dendron and 9-acid dendron, respectively, contributed to achieve *ca.* 83% probability of getting the single-peaked force−distance curve. In comparison, the high-density substrate surface showed *ca.* 45% probability, even with the dendron-modified AFM tip. The higher probability of the single-peaked unbinding event ensured more frequent formation of the single DNA duplex with a nick when the AFM tip approached the substrate surface. Because it is a prerequisite to form a single-nicked DNA duplex reliably for the observation and validation of a nick-sealing reaction at a single nick, the control of lateral spacing on both surfaces is essential.

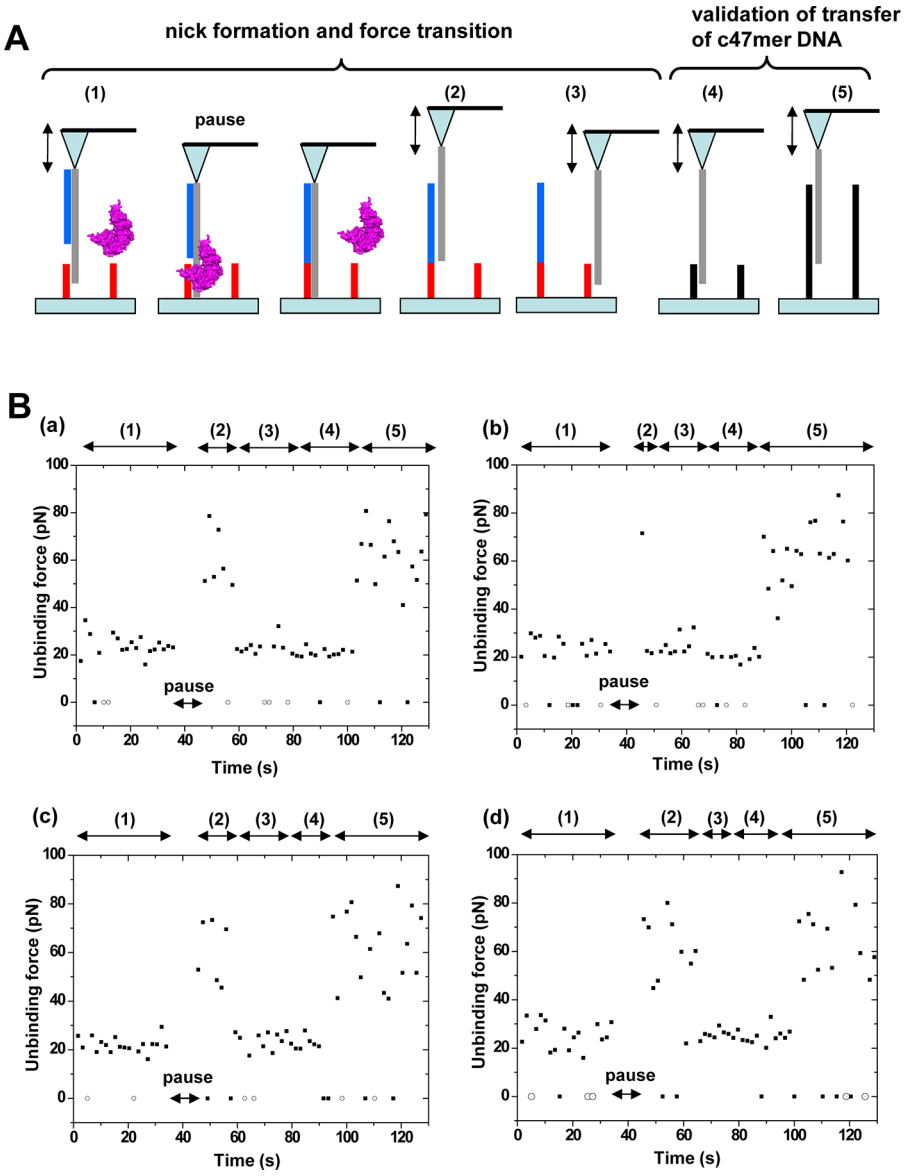

Figure 2. Transition of the unbinding force before and after the single nick-sealing event. (A) Schematic illustration of the force transition due to the single nick-sealing and force validation after nick-sealing. After confirming the presence of c24mer (5′-PO_4) DNA on the 9-acid dendron surface using the AFM tip with 71mer/c47mer DNA (1), the AFM tip was paused at the point and was retracted for the force measurement (2). The AFM tip could be laterally drifted to a neighboring c24mer (5′-PO_4) DNA upon repeated force spectroscopy (3). To confirm the transfer of c47mer DNA from the 71mer DNA during the nick-sealing event, the AFM tip was moved to the c24mer (5′-OH) (4) and c71mer DNAs (5) sequentially for force measurement on the spotted substrate surface. (B) Change in the unbinding force along the lapsed time in four different runs (a to d). The legends (1 to 5) at the top of the profile correspond to the legends in (A). The filled square and open circle at the level of 0 pN indicate the no binding event and nonspecific interaction, respectively.

In this work, T4 DNA ligase was employed since it is widely used for *in vitro* ligation applications, and the reaction temperature employed here (25 °C) was close to known examples (16 and 37 °C).[27,28] To better understand its behavior on the dendron-modified surface, a fluorophore-tagged c24mer (5′-PO_4) DNA was incubated at 25 °C in the presence of 1.2 μM T4 DNA ligase, and the 71mer/c47mer DNA was immobilized onto the surface. The fluorescence intensity reached 25% and 65% of the level-off in 10 and 30 s, respectively, and saturated in 120 s.

To monitor the nick-sealing reaction (Figure 2A), first, an AFM tip tethering hybridized 71mer/c47mer DNA approached the substrate surface where c24mer (5′-PO_4) DNA was immobilized (stage 1). If the unbinding event at one point showed a single-peaked curve, and its unbinding force was within the same range as the 24-bp DNA duplex, the point was considered a candidate site for the single nick-sealing event. The AFM tip was paused at the point to allow DNA ligase to recognize and seal the nick in the ligation solution. After the pause, the AFM tip was retracted and the

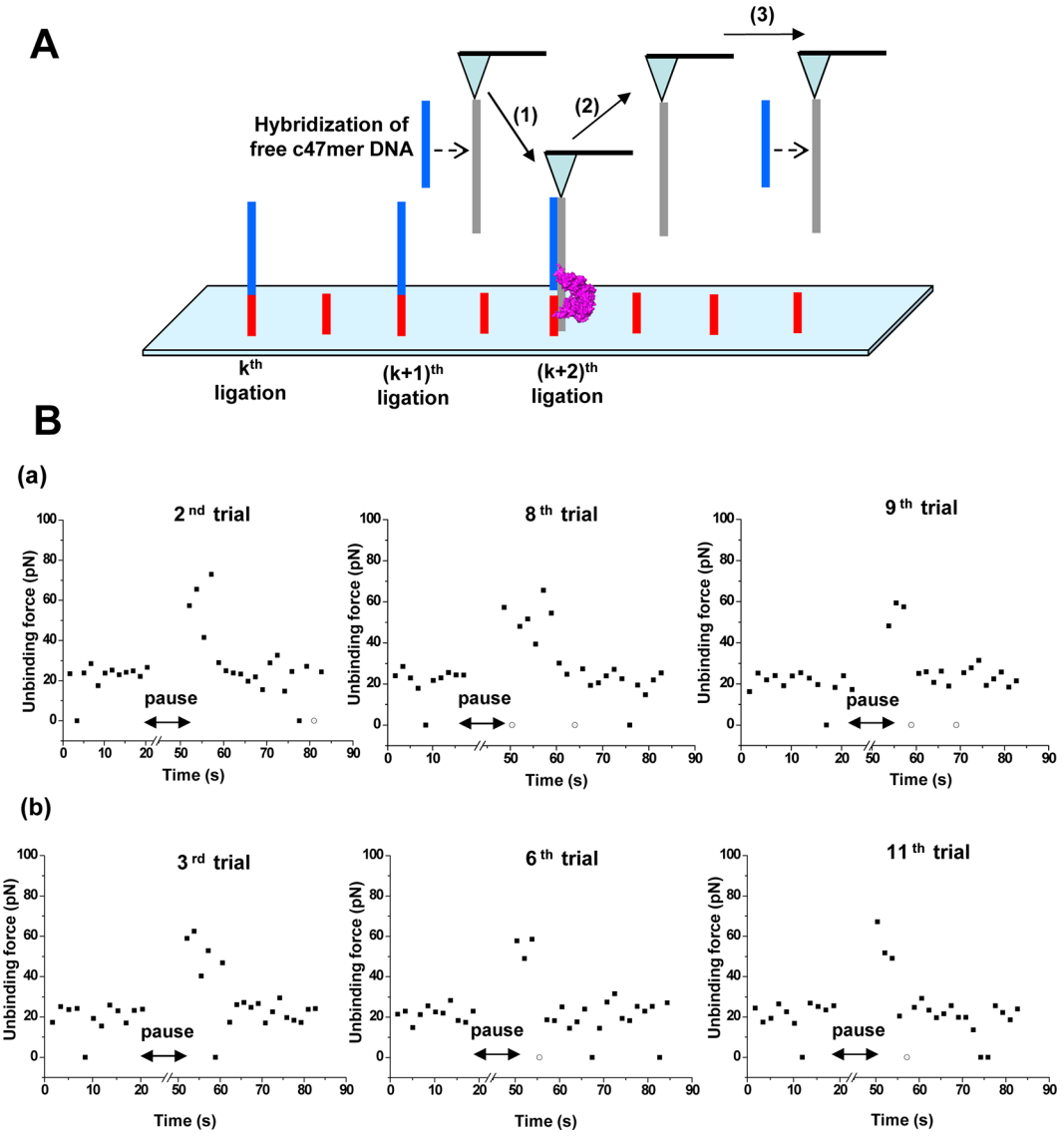

Figure 3. Successive nick-sealing. (A) Schematic illustration of successive nick-sealing at different positions. The free c47mer DNA (1 μM) in ligation solution was hybridized to the 71mer DNA (step 1) prior to the single nick-sealing event (step 2). After ligation, the AFM tip was moved to a new position for the next nick-sealing event (step 3). (B) Profiles of the unbinding force were included only when the expected force increase was detected during the successive trials at different positions. (a) Three force transitions out of 10 successive trials. (b) Three force transitions out of 15 successive trials. The filled square and open circle at the level of 0 pN indicate the no binding event and nonspecific interaction, respectively.

unbinding force was measured. The unbinding force increased from 24.0 ± 4.4 pN (stage 1) to 62.8 ± 14.6 pN (stage 2) after the pause (Figure 2B). Upon repeated measurements, the unbinding force decreased to 22.4 ± 2.3 pN within tens of seconds (stage 3). For validation, the unbinding forces of the c24mer (5′-OH) and c71mer were measured separately by moving the AFM tip to neighboring spots where two types of complementary ssDNAs were immobilized. The mean force values were 23 ± 4 and 65 ± 14 pN (stages 4 and 5), respectively. The unbinding force value at each stage is summarized in Table S2. When force transitions were not observed, the unbinding force value with respect to the c71mer DNA was measured to check the intactness of the AFM tip. A force value less than 35 pN indicated that the ligation did not occur within the pause time while the AFM tip was intact. As a control, the AFM tip with 71/c47mer-hybridized DNA was paused on the c24mer (5′-OH) DNA in the presence of DNA ligase and retracted repeatedly. No increase in the force after the pause time was observed due to the absence of a phosphate group at the 5′ end of the c24mer (Figure S3).

When the pause time for the single nick-sealing was extended from 10 s to 30 s, the probability of observing the force transition increased to 60%, while the probability for the 10 s pause was 23%. Increasing the pause time to 120 s did not enhance the probability. The success yields of 10 and 30 s matched well with the yield observed in solution phase, but did not reach

100% at 120 s. This behavior can be explained by the thermal drift of the AFM under the employed conditions. While the ligase must have sufficient time to complete the reaction, the drift causing the template DNA to move beyond the hydrodynamic radius of the c24mer DNA on the substrate surface could be problematic. Therefore, one must reduce the drift and provide sufficient reaction time (*e.g.*, 120 s) to make the yield 100%. Nevertheless, this observation indicates that it is possible to use AFM to follow kinetic behaviors at the single-molecule level, as long as the reaction is fast enough not to be limited by the drift. Previously, radioisotope or fluorescence labeling was employed to understand the ensemble-averaged kinetics of the nick-sealing event.[27,29] Tang *et al*. utilized a molecular beacon to monitor the ensemble ligation in real time.[30] Our label-free detection of the single nick-sealing event *via* AFM established an experimental procedure to directly monitor and validate the single DNA ligation without any labeling, amplification, or separation.

Instead of employing an AFM tip tethering hybridized 71mer/c47mer DNA, an AFM tip tethering only 71mer DNA was utilized for ligations at multiple points in a batch reaction (Figure 3A). The AFM tip was immersed in the ligation solution containing free c47mer DNA. The 71mer DNA on the AFM tip was expected to hybridize with the c47mer DNA in solution, and after the nick-sealing event, the AFM tip can be reused for ligation at a new position. Because 1 min was sufficient for the hybridization between two DNAs, at least 1 min was allowed before the AFM tip was brought to the c24mer DNA for ligation. Figure 3B shows two representative cases in which the successive ligations occurred. In the first case, the increase in the unbinding force was observed at trial numbers 2, 8, and 9 out of 10 total trials. In the second case, the approach worked for trial numbers 3, 6, and 11 out of 15 total trials (Figure 3B). In all cases, the unbinding force returned to ~23 pN from ~60 pN within 10 s after the ligation-induced force transition. The successive ligation at different positions could be a way for positive patterning with single-molecule precision, although optimizing the conditions considering the drift is necessary. Also, it is not clear why the yield decreased from 60% to 30% or less in the successive ligation, although a 30 s pause time was allowed in all trials. Free c47mer DNA in solution may be able to deter the binding and ligation reactivity of the T4 DNA ligase.

The shorter duration time of the increased force was observed in the successive ligation. The increased force in the nonsuccessive ligation lasted 17.9 ± 8.0 s before returning to the force value of the 24-bp DNA, whereas it took 5.7 ± 2.8 s in the successive ligation (Figure S4). Because the free c47mer DNA in the successive ligation could hybridize with the 71mer DNA on the AFM tip during the postligation force measurement stage, the faster reduction of the unbinding force in the successive ligation seems reasonable. Moreover, the profile of duration time in the successive ligation fit with an exponential decay, whereas the profile in the nonsuccessive ligation fit with the Gaussian curve. The former exponential decay is indicative of first-order kinetics characterized by the binding of c47mer DNA to the 71mer template DNA.

Successive nick-sealing with AFM can be expected to allow one to covalently build up or pattern DNA-based nanostructures at defined points. Our bottom-up approach is a positive patterning method at a nanoscale, which is in contrast to the negative patterning that utilizes the substrate-converting enzyme immobilized on the AFM tip.[4] The AFM-based successive ligation of free nanoparticle−DNA conjugates as a molecular ink has the potential to implement high-resolution nanowriting. Therefore, it is necessary to understand the other details associated with the ligation and to optimize the mechanical and biochemical conditions accordingly.

CONCLUSIONS

In summary, the enzymatic single nick-sealing event in a single DNA duplex can be directly detected and validated by monitoring the transition of the unbinding force by AFM. The dendron modification of the AFM tip and substrate surface allows the reliable formation of a single nick in a DNA duplex due to the controlled lateral spacing for the immobilized DNA strands. This approach may be applied to study other enzymatic reactions at the single-molecule level and to generate bottom-up nanostructures on the surface.

EXPERIMENTAL METHODS

Materials. Dendron-modified glass slides were obtained from NSB POSTECH (Seoul, Korea). SuperAmine (high-density amine) glass slides were purchased from Arrayit (Sunnyvale, CA, USA). T4 DNA ligase (400 U/μL, 12 μM) and adenosine triphosphate (ATP, 100 mM in stock, purity of >96% by HPLC) were acquired from Solgent (Daejeon, Korea) and Fermentas (Glen Burnie, MD, USA), respectively, and stored at −20 °C until use. Single-stranded nucleotides (Table S3) were purchased from Bioneer (Daejeon, Korea). AFM probes were obtained from NanoInk (Skokie, IL, USA). All chemicals and solvents of reagent grade were purchased from Sigma-Aldrich (St. Louis, MO, USA) unless otherwise mentioned. Ultrapure deionized (DI) water (18.2 MΩ·cm) was obtained by use of a Milli-Q purification system (Millipore, Billerica, MA, USA).

Immobilization of Oligonucleotides on an AFM Tip. AFM probes (a tip radius of ~15 nm, a gold film for the laser reflection, and a nominal spring constant of 16 pN/nm, DPN Probe: type B, NanoInk) were modified with a 27-acid dendron (Figure S5) molecule as described previously.[31] Prior to the covalent

immobilization of the amine-modified oligonucleotides, *N*,*N*′-disuccinimide carbonate (DSC) was conjugated on the surface of the AFM tip as a cross-linker. A prepared *N*-hydroxysulfosuccinimide (NHS)-functionalized AFM tip was incubated in a spotting buffer (25 mM sodium bicarbonate, 5 mM $MgCl_2$, and 10% (v/v) dimethyl sulfoxide, pH 8.5) containing 3′-NH_2-modified 71mer DNA (20 μM) at 25 °C for 12 h, washed with washing buffer (300 mM NaCl, 20 mM Na_2HPO_4, 2 mM ethylenediaminetetracetic acid, and 7 mM sodium dodecyl sulfate (SDS)), rinsed carefully in DI water, and dried under vacuum (~100 mTorr) for 30 min. For the hybridization of c47mer DNA with the tethering 71mer DNA, the AFM probe was incubated in a hybridization buffer (300 mM NaCl, 2 mM Na_2HPO_4, 2 mM EDTA, 7 mM SDS, pH 7.4) containing 2 μM c47mer DNA in an 80% humidity chamber for 12 h at 25 °C. The resulting AFM probe was washed with washing buffer and rinsed with DI water.

Preparation of the Substrate Surface. The conjugation of DSC to the amine group on the high-density amine or 9-acid dendron-modified glass slides was performed as described previously.[32] The 3′-NH_2-modified ssDNAs were dissolved in the spotting buffer, and the concentration was adjusted to 15 μM for immobilization onto the NHS surface. The dissolved ssDNA was spotted onto the glass slide using a contact-type microarrayer (QArray mini; Genetix, New Milton, UK) (Figure S6). Printed slides were incubated in an 80% humidity chamber for 12 h. The slides were washed with saline–sodium citrate buffer (150 mM NaCl, 15 mM sodium citrate, 0.2% SDS) to remove unbound DNAs. The slides were then rinsed with water and dried by centrifugation at 200*g* for 3 min at room temperature.

Measurement of Unbinding Forces for Hybridized DNAs. Force–displacement curves were recorded by NanoWizard AFM (JPK Instruments, Berlin, Germany) on an inverted optical microscope (Axiovert 200; Carl Zeiss, Oberkochen, Germany). The combined AFM system was set on an antivibration table and electromagnetically shielded to minimize the external perturbation during force recording. The DNA-tethered AFM probe and substrate slide were installed in the AFM head and stage, respectively. Then 200 μL of 1× ligation buffer (30 mM Tris-HCl, 10 mM $MgCl_2$, 10 mM 1,4-dithiothreitol, 1 mM ATP, pH 7.8) was slowly injected into a gap between the AFM probe and substrate. The spring constant of each cantilever was determined in the ligation buffer at 25 °C by using the NanoWizard program (thermal noise method). The AFM tip approached the substrate surface and retracted at a cycle of 1.8 s along the initial *z*-length (the movable displacement of an AFM tip in the vertical direction) of 450 nm to obtain the force–distance curves at a defined point (*i.e.*, constant velocity mode of 0.50 μm/s). All force–distance curves were classified into five groups according to their shape and number of peaks: nonspecific, no binding, single-peaked, double-peaked, and multipeaked (more than three peaks) curves (Figure S7). The nonspecific unbinding curves were excluded for further analysis, and the curves with indistinguishable peaks from the noise level were counted as no binding.

***In Situ* Detection of Single Nick-Sealing Events.** After placing an AFM tip over a point within the c24mer DNA spot, the measurements were repeated at various points until the specific force value showing the interaction between c24mer and 71mer/c47mer DNAs was observed (Figure S8). The *z*-length was limited to ~20 nm near the substrate surface, and the AFM tip was allowed to approach and retract at a point on the substrate surface. During a retraction cycle, the movement of the AFM tip was stopped near the baseline, and a certain pause time (10, 30, or 120 s) was allowed in the presence of 1.2 μM T4 DNA ligase (40 U/μL) in ligation buffer containing 1 mM ATP. After the pause, the AFM tip was retracted and the unbinding force was recorded. The repeated force measurement cycle was performed until an increase in the unbinding force was observed. Finally, the AFM tip was moved to the c24mer (5′-OH) and c71mer spots sequentially, and the unbinding forces were recorded to confirm the transfer of c47mer DNA from the AFM tip to a c24mer DNA (5′-PO_4) in the ligation.

Analysis of Force–Distance Curves. The force–distances curves automatically stored during the force measurement were viewed with a JPK image processing program (SPM IP, ver. 3.1.15). The unbinding force was defined as the difference in the force between the peak of a force–distance curve and the baseline. The histogram for the no binding and specific unbinding events was obtained by collecting force–distance curves (more than 100 curves per point) at several different points (more than five points in a spot region). The nonspecific force–distance curves were eliminated in the histogram. The last peak in the double-peaked or multiple-peaked curve was read as a valid unbinding force. The representative force–distance curves were reconstructed by OriginPro v7.5 (OriginLab, Northampton, MA, USA). With the bin size of 5 pN, the histogram for the unbinding event obtained at a given condition was fitted to a Gaussian curve to estimate the most probable unbinding force value and standard deviation. The force value transition due to the single nick-sealing event was plotted as a function of time.

Conflict of Interest: The authors declare no competing financial interest.

Acknowledgment. This study was supported by the World Class University (WCU) program through the National Research Foundation (NRF) of Korea funded by the Ministry of Education, Science and Technology (MEST, grant number R31-2008-000-10105-0) and BK21. The authors acknowledge the financial support from the Converging Research Center Program through the National Research Foundation of Korea funded by MEST (grant numbers 2011K000801, 2012-0001135). The authors are grateful to Ji Hye Shin and Yeon Jeong Seok for their help in inputting the analyzed unbinding force values. We also thank Youngkyu Kim for giving useful suggestions during the revision.

Supporting Information Available: Additional information about the DNA sequence, surface modification, force measurement, distribution of unbinding forces, and characteristics of force transition is provided. This material is available free of charge *via* the Internet at http://pubs.acs.org.

REFERENCES AND NOTES

1. Binnig, G.; Quate, C. F.; Gerber, C. Atomic Force Microscope. *Phys. Rev. Lett.* **1986**, *56*, 930–933.
2. Muller, D. J.; Dufrene, Y. F. Atomic Force Microscopy as a Multifunctional Molecular Toolbox in Nanobiotechnology. *Nat. Nanotechnol.* **2008**, *3*, 261–269.
3. Luo, X. L.; Pedrosa, V. A.; Wang, J. Enzymatic Nanolithography of Polyaniline Nanopatterns by Using Peroxidase-Modified Atomic Force Microscopy Tips. *Chem.—Eur. J.* **2009**, *15*, 5191–5194.
4. Riemenschneider, L.; Blank, S.; Radmacher, M. Enzyme-Assisted Nanolithography. *Nano Lett.* **2005**, *5*, 1643–1646.
5. Hyun, J.; Kim, J.; Craig, S. L.; Chilkoti, A. Enzymatic Nanolithography of a Self-Assembled Oligonucleotide Monolayer on Gold. *J. Am. Chem. Soc.* **2004**, *126*, 4770–4771.
6. Ionescu, R. E.; Marks, R. S.; Gheber, L. A. Nanolithography Using Protease Etching of Protein Surfaces. *Nano Lett.* **2003**, *3*, 1639–1642.
7. Takeda, S.; Nakamura, C.; Miyamoto, C.; Nakamura, N.; Kageshima, M.; Tokumoto, H.; Miyake, J. Lithographing of Biomolecules on a Substrate Surface Using an Enzyme-Immobilized AFM Tip. *Nano Lett.* **2003**, *3*, 1471–1474.
8. Piner, R. D.; Zhu, J.; Xu, F.; Hong, S. H.; Mirkin, C. A. "Dip-Pen" Nanolithography. *Science* **1999**, *283*, 661–663.
9. Kumar, A.; Whitesides, G. M. Features of Gold Having Micrometer to Centimeter Dimensions Can Be Formed through a Combination of Stamping with an Elastomeric Stamp and an Alkanethiol "Ink" Followed by Chemical Etching. *Appl. Phys. Lett.* **1993**, *63*, 2002–2004.
10. Braunschweig, A. B.; Huo, F. W.; Mirkin, C. A. Molecular Printing. *Nat. Chem.* **2009**, *1*, 353–358.
11. Salaita, K.; Wang, Y. H.; Mirkin, C. A. Applications of Dip-Pen Nanolithography. *Nat. Nanotechnol.* **2007**, *2*, 145–155.
12. Tinazli, A.; Piehler, J.; Beuttler, M.; Guckenberger, R.; Tampe, R. Native Protein Nanolithography that Can Write, Read and Erase. *Nat. Nanotechnol.* **2007**, *2*, 220–225.

13. Zhu, R.; Howorka, S.; Proll, J.; Kienberger, F.; Preiner, J.; Hesse, J.; Ebner, A.; Pastushenko, V. P.; Gruber, H. J.; Hinterdorfer, P. Nanomechanical Recognition Measurements of Individual DNA Molecules Reveal Epigenetic Methylation Patterns. *Nat. Nanotechnol.* **2010**, *5*, 788–791.
14. Husale, S.; Persson, H. H. J.; Sahin, O. DNA Nanomechanics Allows Direct Digital Detection of Complementary DNA and microRNA Targets. *Nature* **2009**, *462*, 1075–1078.
15. Struckmeier, J.; Wahl, R.; Leuschner, M.; Nunes, J.; Janovjak, H.; Geisler, U.; Hofmann, G.; Jahnke, T.; Muller, D. J. Fully Automated Single-Molecule Force Spectroscopy for Screening Applications. *Nanotechnology* **2008**, *19*, 1–10.
16. Zhang, W.; Lü, X.; Zhang, W. K.; Shen, J. EMSA and Single-Molecule Force Spectroscopy Study of Interactions between *Bacillus subtilis* Single-Stranded DNA-Binding Protein and Single-Stranded DNA. *Langmuir* **2011**, *27*, 15008–15015.
17. Cao, Y.; Li, H. B. Dynamics of Protein Folding and Cofactor Binding Monitored by Single-Molecule Force Spectroscopy. *Biophys. J.* **2011**, *101*, 2009–2017.
18. Liang, J.; Fernandez, J. M. Kinetic Measurements on Single-Molecule Disulfide Bond Cleavage. *J. Am. Chem. Soc.* **2011**, *133*, 3528–3534.
19. Bustamante, C.; Macosko, J. C.; Wuite, G. J. Grabbing the Cat by the Tail: Manipulating Molecules One by One. *Nat. Rev. Mol. Cell Biol.* **2000**, *1*, 130–136.
20. Kufer, S. K.; Puchner, E. M.; Gumpp, H.; Liedl, T.; Gaub, H. E. Single-Molecule Cut-and-Paste Surface Assembly. *Science* **2008**, *319*, 594–596.
21. Kufer, S. K.; Strackharn, M.; Stahl, S. W.; Gumpp, H.; Puchner, E. M.; Gaub, H. E. Optically Monitoring the Mechanical Assembly of Single Molecules. *Nat. Nanotechnol.* **2009**, *4*, 45–49.
22. Jung, Y. J.; Hong, B. J.; Zhang, W.; Tendler, S. J.; Williams, P. M.; Allen, S.; Park, J. W. Dendron Arrays for the Force-Based Detection of DNA Hybridization Events. *J. Am. Chem. Soc.* **2007**, *129*, 9349–9355.
23. Kim, D.; Chung, N. K.; Kim, J. S.; Park, J. W. Immobilizing a Single DNA Molecule at the Apex of AFM Tips through Picking and Ligation. *Soft Matter* **2010**, *6*, 3979–3984.
24. Kim, D.; Chung, N. K.; Allen, S.; Tendler, S. J.; Park, J. W. Ferritin-Based New Magnetic Force Microscopic Probe Detecting 10 nm Sized Magnetic Nanoparticles. *ACS Nano* **2012**, *6*, 241–248.
25. Armstrong, J.; Brown, R. S.; Tsugita, A. Primary Structure and Genetic Organization of Phage T4 DNA Ligase. *Nucleic Acids Res.* **1983**, *11*, 7145–7156.
26. Shuman, S. DNA Ligases: Progress and Prospects. *J. Biol. Chem.* **2009**, *284*, 17365–17369.
27. Cherepanov, A. V.; de Vries, S. Kinetics and Thermodynamics of Nick Sealing by T4 DNA Ligase. *Eur. J. Biochem.* **2003**, *270*, 4315–4325.
28. Lohman, G. J.; Chen, L.; Evans, T. C., Jr. Kinetic Characterization of Single Strand Break Ligation in Duplex DNA by T4 DNA Ligase. *J. Biol. Chem.* **2011**, *286*, 44187–44196.
29. Bullard, D. R.; Bowater, R. P. Direct Comparison of Nick-Joining activity of the Nucleic Acid Ligases from Bacteriophage T4. *Biochem. J.* **2006**, *398*, 135–144.
30. Tang, Z.; Wang, K.; Tan, W.; Li, J.; Liu, L.; Guo, Q.; Meng, X.; Ma, C.; Huang, S. Real-Time Monitoring of Nucleic Acid Ligation in Homogenous Solutions Using Molecular Beacons. *Nucleic Acids Res.* **2003**, *31*, e148.
31. Roy, D.; Kwon, S. H.; Kwak, J. W.; Park, J. W. "Seeing and Counting" Individual Antigens Captured on a Microarrayed Spot with Force-Based Atomic Force Microscopy. *Anal. Chem.* **2010**, *82*, 5189–5194.
32. Hong, B. J.; Oh, S. J.; Youn, T. O.; Kwon, S. H.; Park, J. W. Nanoscale-Controlled Spacing Provides DNA Microarrays with the SNP Discrimination Efficiency in Solution Phase. *Langmuir* **2005**, *21*, 4257–4261.